Electronic excited-state wave functions for quantum Monte Carlo: Application to silane and methane

A. R. Porter, O. K. Al-Mushadani, M. D. Towler, and R. J. Needs[a)]
TCM Group, Cavendish Laboratory, University of Cambridge, Madingley Road, Cambridge, CB3 0HE, United Kingdom

(Received 7 November 2000; accepted 1 December 2000)

We investigate the efficient construction of guiding wave functions for use in diffusion Monte Carlo calculations of electronic excited states. We test guiding wave functions obtained from singles-only configuration interaction, time-dependent density functional theory, and complete active space self-consistent field methods. The techniques are used to study the first ionization potentials and excited states of silane and methane. © *2001 American Institute of Physics.*
[DOI: 10.1063/1.1342765]

I. INTRODUCTION

The electronic excited states of molecules and larger clusters are of great technological importance. One would like to be able to predict the optical absorption/emission spectra of any given molecular structure, but excitation energies have proved more difficult to calculate than ground-state energies. In this paper we study the singly ionized and neutral excited states of silane and methane using the fixed-node diffusion quantum Monte Carlo (DMC) method.[1] Silane and methane are good benchmarking systems as they have been well studied, both experimentally[2,3] and theoretically.[4–9] Our DMC results are in good agreement with the best results obtained in other calculations, where available, but the comparison with experiment is not straightforward, especially for the vertical transitions. The possible role of Jahn–Teller distortions and vibrational structure is discussed in accounting for the apparent discrepancies between the theoretical and experimental results.

DMC presents an attractive approach for studying electronic systems because of its potentially high accuracy and the favorable scaling of the computational cost with system size. Very accurate calculations of ground-state energies have already been demonstrated and in principle such performance can also be attained for excited states. The accuracy of a DMC calculation is determined by the quality of the nodal surface of the guiding wave function. Therefore, we require an affordable and reasonably accurate method for generating excited-state guiding wave functions. Grimes *et al.*[10] used multiconfiguration self-consistent field calculations (MCSCF) to generate a guiding wave function for an excited state of H_2; more recently, Grossman *et al.*[8] have used a similar approach for the silane and methane molecules. The drawback of this approach is that MCSCF calculations are themselves expensive and cannot be applied to large systems. In this paper, we examine the usefulness of singles-only CI (CIS) and time-dependent density-functional theory (TD-DFT) as cheaper methods of generating excited-state guiding wave functions.

Many computational methods have been used to study excited states. Density-functional theory (DFT) and Hartree–Fock (HF) theory are very successful for calculating ground-state properties, but they often provide a poor description of excited states. Many powerful quantum chemistry techniques such as configuration interaction (CI) and coupled cluster methods are applicable to excited states.[11] High quality quantum chemistry calculations have been reported by Chantranupong *et al.*[6] for excited states of silane and by Mebel *et al.*[9] for methane. Although these methods can produce very accurate results, the computational cost increases very rapidly with the system size and they are therefore limited to small molecules. An alternative approach is that of many-body perturbation theory. For one-body excitations such as ionization energies, techniques based on Hedin's *GW* approximation[12] have proved successful. In optical absorption the electron–hole interaction can be included by solving the Bethe–Salpeter equation (BSE) which involves the two-particle Green's function.[7,13] This *GW*-BSE approach has recently been applied to hydrogen-terminated silicon clusters, including silane.[7,8] Another technique which is gaining in popularity for studying excited states is TD-DFT.[14–18] This method has been applied to hydrogen-terminated silicon clusters, including silane, by Vasiliev *et al.*[19]

II. METHODS

A. The diffusion quantum Monte Carlo method

DMC is a stochastic method for evolving a wave function according to the imaginary-time Schrödinger equation. The imaginary-time evolution projects out the ground-state component from the starting state. However, because the imaginary-time evolution is stochastic and therefore inexact, the solution converges to the overall ground state, which is bosonic. In practical calculations the fermionic symmetry is maintained by the fixed-node approximation,[20] in which the nodal surface of the wave function is constrained to equal that of a guiding wave function. The imaginary-time evolution is accomplished using a density of ''walkers,'' each of which corresponds to a configuration of the system, i.e., to a

a)Electronic mail: rn11@phy.cam.ac.uk

set of electron positions. It has been shown[21,22] that the fixed-node DMC energy provides a variational upper bound on the ground-state energy with an error that is second order in the error in the nodal surface.

The fixed-node constraint also allows us to study excited states. The DMC algorithm converges to the lowest energy state consistent with the fixed nodal surface, and if we use a guiding wave function whose nodal surface approximates that of an excited state then the DMC energy will normally be a good approximation to the energy of the excited state. It is straightforward to show that the DMC algorithm gives the exact energy of an excited state if the fixed nodal surface is exact. However, for excited states, the existence of a variational principle is dependent upon the symmetry of the guiding wave function.[23]

The guiding wave function introduces importance sampling, and therefore its accuracy controls the statistical efficiency of the algorithm and, via the fixed-node approximation, determines the final accuracy that can be obtained. The repeated evaluation of the guiding wave function and its gradient and Laplacian are the most costly parts of the calculation and it is therefore necessary to use guiding wave functions which can be computed rapidly. For ground states of closed-shell systems a single-determinant wave function constructed from orbitals obtained from a standard, self-consistent field calculation (e.g., Hartree–Fock) is normally perfectly adequate. Unfortunately, the same is not generally true of excited states and we must move to more sophisticated methods in order to obtain guiding wave functions with good nodal surfaces.

The guiding wave functions used in our calculations are of the Slater–Jastrow form

$$\Psi(\{\mathbf{r}\}) = \left(\sum_i^{N_{\mathrm{det}}} c_i \mathcal{D}_i^{\uparrow} \mathcal{D}_i^{\downarrow} \right) \exp(\mathcal{J}), \tag{2.1}$$

where $\{\mathbf{r}\} = \{\mathbf{r}_1, \mathbf{r}_2, \ldots, \mathbf{r}_{N_e}\}$ is the set of positions of all N_e electrons, $\exp(\mathcal{J})$ is a Jastrow factor,[24] and the $\mathcal{D}_i^{\uparrow}/\mathcal{D}_i^{\downarrow}$ are Slater determinants of one-particle up-/down-spin orbitals. The Jastrow factor is positive and multiplicative and does not alter the nodes of the wave function which are therefore fixed by the determinantal part. The determinants, along with their associated coefficients, c_i, may be obtained using a variety of methods as discussed in Sec. II B. Throughout this paper we denote a DMC calculation using a guiding wave function obtained from a particular *method* by DMC(*method*).

In the calculations presented here, we use a Jastrow factor of the form[25]

$$\mathcal{J} = -\sum_{i \neq j}^{N_e} [U_0(r_{ij}) + U(r_{ij})] + \sum_k^{N_n} \sum_i^{N_e} S_k(r_{ik}), \tag{2.2}$$

where N_n and N_e are the number of atomic nuclei and electrons, respectively. The function U_0 is chosen such that the wave function obeys the cusp conditions[26] which apply at a two-electron coalescence. We express both U and S_k as polynomial expansions in the inter-particle distances. Variance minimization techniques[27,28] are used to find the optimum values of the parameters in the Jastrow factor.

B. Construction of excited-state guiding wave functions

As described in the previous section, using DMC to calculate an accurate total energy hinges on our ability to obtain a guiding wave function with a nodal surface that is as close as possible to that of the state of interest. The aim here is to take a readily affordable quantum chemistry technique, namely singles-only configuration interaction (CIS),[29] and investigate whether the resulting improvement in the nodal surface is sufficient to allow accurate DMC calculations.

1. CIS wave functions and resumming

The CIS method is based on constructing a wave function from determinants which involve only single excitations from the HF ground-state determinant

$$|\Psi\rangle = \sum_a^{N_e} \sum_r^{N_v} c_a^r |S_a^r\rangle. \tag{2.3}$$

The configurations $|S_a^r\rangle$ represent single-electron excitations where an electron has been removed from occupied orbital a (of which there are N_e) and put into virtual orbital r (of which there are N_v). The expansion coefficients, c_a^r, are determined by solving the Schrödinger equation in the basis of the singly excited determinants.

Although the CIS wave function neglects all correlation effects due to double and higher excitations, the approach has considerable merit. The CIS wave functions are orthogonal to the ground-state HF determinant and therefore CIS is a rather natural extension of HF theory to excited states. The variational determination of the expansion coefficients allows relaxation of the entire wave function in the presence of the excitation, so that it includes a reasonable description of electron–hole interactions. For excitations from a closed-shell ground state, the CIS wave functions are pure singlets and triplets. CIS is also a size-consistent theory.[29] The CIS method is fairly inexpensive and should be applicable to quite large systems. Another factor which is important for using CIS wave functions within DMC is that the CIS wave function can be handled very efficiently using the simple resumming technique described below.

If the ground state of the system contains N_e occupied spin orbitals and we include N_v virtual or unoccupied states, there are $N_e \times N_v$ possible singly excited determinants. We write a determinant as

$$\mathcal{D} = \begin{vmatrix} \phi_1(\mathbf{r}_1) & \phi_2(\mathbf{r}_1) & \cdots & \phi_{N_e}(\mathbf{r}_1) \\ \phi_1(\mathbf{r}_2) & \phi_2(\mathbf{r}_2) & & \\ \vdots & & \ddots & \\ \phi_1(\mathbf{r}_{N_e}) & & & \phi_{N_e}(\mathbf{r}_{N_e}) \end{vmatrix} = |1\,2 \cdots N_e|.$$

Each orbital appears only once in each of the $N_e!$ terms which make up the determinant. Therefore, we can add together two determinants which differ only in a single orbital, e.g.,

$$|1\,2 \cdots N_e| + |1\,2' \cdots N_e| = |1(2+2') \cdots N_e|. \tag{2.4}$$

Consequently, the N_v determinants obtained by exciting from a particular orbital may be resummed into a single determinant. Since there are N_e orbitals to excite from, we can resum the entire CIS wave function into N_e determinants. This represents a considerable saving in the amount of storage and computation required when using such a wave function in a DMC calculation. For instance, the CIS expansion for the first singlet excited state of silane considered in Sec. III C 1 contains 384 determinants. As silane in a pseudopotential calculation has eight electrons, this wave function may be resummed into just eight determinants.

2. Spin eigenfunctions

In order to construct determinantal wave functions which are eigenstates of the spin operators $\hat{S}_z$ and $\hat{S}^2$, it is necessary to ensure that the spin parts of such wave functions are themselves either symmetric (for triplets) or antisymmetric (for singlets) with respect to particle exchange. If we consider an excitation from spatial orbital a to spatial orbital r, then the desired singlet state may be constructed according to

$$|^1S_a^r\rangle = \frac{1}{\sqrt{2}}(|S_a^r\rangle + |S_{\bar{a}}^{\bar{r}}\rangle). \tag{2.5}$$

Here, $|S_a^r\rangle = (1/\sqrt{N_e})\mathcal{D}_a^r$ denotes the excitation of a spin-up electron from orbital a to orbital r and $|S_{\bar{a}}^{\bar{r}}\rangle$ is that for a spin-down electron. There are three different triplet states corresponding to the three possible values $(1, 0, -1)$ of S_z. We choose to form the triplet with $S_z = 0$

$$|^3S_a^r\rangle = \frac{1}{\sqrt{2}}(|S_{\bar{a}}^{\bar{r}}\rangle - |S_a^r\rangle). \tag{2.6}$$

3. Other forms of guiding wave function

In order to study the quality of the nodal surface of the CIS wave functions, we have also performed some calculations with the more accurate (and much more expensive) complete active space multiconfiguration self-consistent field (CASSCF) method.[30] Unlike CIS, where only single excitations are considered, in CASSCF one constructs all possible excited configurations within a given ''active space.'' This active space will in general consist of the highest few occupied molecular orbitals, combined with a certain number of the lowest unoccupied molecular orbitals. In addition the molecular orbitals themselves are also optimized during the calculation. CASSCF is therefore potentially a very accurate method, but it is very expensive. The number of configurations that must be considered increases very rapidly with the size of the active space, which must therefore be somewhat limited. From the DMC point of view, CASSCF also suffers the disadvantage that the number of determinants that can be resummed is rather limited because the wave function contains doubly- and higher-excited determinants.

As well as the above methods, we have also used wave functions obtained from TD-DFT calculations,[14–18] which have been shown to produce good results for small molecules.[31,32] The calculation of electronic excitation energies within TD-DFT makes use of linear-response theory within the time-dependent density-functional formalism.[15] The excitation energies are obtained by calculating the poles in the dynamic polarizability of the system and the corresponding wave functions may be approximated by expansions in particle–hole pairs.[17] This is the same as the form of wave function obtained from a CIS calculation and therefore may also be fully resummed for use in DMC. In the calculations presented here, we use time-dependent density functional theory within the adiabatic local density approximation and refer to the method as the TD-LDA.

C. Calculation details

Due to the difficulty of dealing with the tightly bound core electrons in DMC,[33] all of the results presented here were obtained using pseudopotentials for the silicon and carbon 4+ ions. The pseudopotentials were generated from the results of all-electron Hartree–Fock atomic calculations using the method of Troullier and Martins.[34,35] This method generates highly transferable pseudopotentials that are also finite at the origin, which helps to reduce time-step errors in the DMC calculations.

The explicit many-body nature of DMC calculations allows the use of core polarization potentials (CPPs)[36] which describe the core–valence correlation effects which are neglected in standard Hartree–Fock calculations. These potentials describe the interaction of the valence electrons with those of the core in terms of classical electrostatics. In the CPP formalism the core–valence correlation is described in terms of the dipole polarization of the core due to the electric field of the valence electrons. In this paper, all of the DMC calculations with the Troullier–Martins HF pseudopotential incorporate CPPs using the formalism and parameters of Shirley and Martin,[37] which also includes relativistic effects. We have also performed some calculations with the Si pseudopotential of Stevens *et al.*,[38] in order to compare with the results of Grossman *et al.*[8]

We use Gaussian basis sets for all of the calculations. For the silicon atom, the basis set consists of 12 uncontracted *s* functions, 6 uncontracted *p* functions, and 2 uncontracted *d* functions. The carbon basis set consists of 12 uncontracted *s* functions, 8 uncontracted *p* functions, and 1 uncontracted *d* function. For silane, the hydrogen basis set consists of 13 uncontracted *s* functions and 2 uncontracted *p* functions. That for methane has three additional *s* functions. Our hydrogen basis sets contain a number of Gaussian *s* functions with very large exponents, which help to give a good description of the orbitals close to the hydrogen nuclei. Although these large-exponent Gaussians play little part in lowering the variational energy, they are important because they reduce the violation of the cusp condition[26] as an electron approaches a nucleus. This helps to stabilize the DMC algorithm.

The exponents of the Gaussians forming these basis sets were first optimized for the ground state of the relevant free atom. Since the interatomic bonding in a molecule alters the optimal form of the basis, the sets were then optimized further in the relevant molecular environment—in this case, the ground states of silane and methane. Care was taken to avoid

TABLE I. Our ground-state and atomization energies, calculated within DMC and using LDA-DFT values for the zero-point energies. Figures in parentheses indicate the standard error in the last decimal place. All energies are in eV.

	DMC ground state energies					Other results		
	X	H	XH_4	Zero-point energy	Atomization energy, D_0	DMC	CCSD(T)	Expt.
SiH_4	−103.03(1)	−13.6057(7)	−171.64(2)	0.806	13.38(2)	13.24(2)[d]	13.19(3)[a]	13.10–13.17[b]
CH_4	−147.74(3)	−13.6057(7)	−220.38(4)	1.167	17.05(5)		17.02[c]	17.021(6)[c]

[a]Feller and Dixon (Ref. 44).
[b]Feller and Dixon (Ref. 44) and references therein.
[c]Martin (Ref. 45) and references therein.
[d]Greeff and Lester (Ref. 43), to which we have added our value of the zero-point energy.

linear dependencies that occur when exponents become equal by ensuring that they remained approximately even tempered. Since the focus of this work is on Rydberg excited states which are considerably more diffuse than ground states, it is important to include diffuse functions in the basis sets. For the hydrogen basis in silane (methane), the minimum *s* exponent is 0.033 (0.01) a.u.^{-2} and the (less important) minimum *p* exponent is 0.543 (0.34) a.u.^{-2}. The corresponding values for the silicon basis are 0.013 and 0.007 a.u.^{-2}, respectively, with the minimum *d* exponent being 0.235 a.u.^{-2}. For carbon, the corresponding values are 0.0025, 0.015, and 1.1 a.u.^{-2}.

All of the CIS, CASSCF, DFT, and TD-LDA calculations presented here were performed using the GAUSSIAN 98 software package,[39] while for the DMC calculations we used the CASINO[40] quantum Monte Carlo code, which can be used for finite or periodic systems in one, two, or three dimensions.

III. RESULTS

A. Ground-state results

The ground states of SiH_4 and CH_4 both have tetrahedral symmetry. Relaxing the structures within LDA-DFT gave a Si–H bond length of 1.505 Å and a C–H bond length of 1.103 Å. These bond lengths are in good agreement with the corresponding experimental values of 1.474 Å[41] and 1.09 Å[42], respectively.

In order to validate the basis set and methods, we have calculated the atomization energies, D_0, of silane and methane. For the molecule XH_4 with X={Si,C}, these are calculated according to

$$D_0 = E_{\text{gs}}(\text{X}) + 4E_{\text{gs}}(\text{H}) - [E_{\text{gs}}(\text{XH}_4) + E_{\text{ZPE}}(\text{XH}_4)],$$

where $E_{\text{gs}}(\text{X})$ is the electronic ground-state energy of X and $E_{\text{ZPE}}(\text{XH}_4)$ is the zero-point energy of the molecule (which we have calculated within the harmonic approximation using LDA-DFT). Table I gives the results of these calculations, along with the relevant ground-state energies. The agreement with both other theoretical calculations and with experiment is reasonable. Our DMC atomization energy of silane of 13.38(2) eV is close to the value of 13.24(2) eV obtained by Greeff and Lester[43] using DMC (we have corrected their value using our zero-point energy). Our result differs from Feller and Dixon's[44] coupled-cluster singles and doubles augmented by a perturbative correction for triples [CCSD(T)] result by only 0.15(4) eV when their value for the zero-point energy is used. Feller and Dixon[44] performed all-electron calculations, with the 1*s* orbital of Si frozen, and used a high-quality basis set. Their final result is an extrapolation to the complete basis-set limit and incorporates core–valence correlation and relativistic corrections including the spin–orbit interaction. The spin–orbit interaction, which is not included in our calculation, reduces D_0 by about 0.02 eV. Our value for the atomization energy of methane is in excellent agreement with the CCSD(T) calculations of Martin[45] and with experiment.

B. Ionization potentials

First, we study the spectrum associated with the first ionization potential (I.P.) of silane and methane. Care must be taken when comparing theoretical results with experiment since two different I.P.s are commonly quoted, vertical and adiabatic. The adiabatic I.P. is defined as the energy needed to ionize a molecule initially in its ground state, with *no change* in the vibrational and rotational quantum numbers. Experimentally, it approximately corresponds to the onset of the peak in the spectrum. The vertical I.P. is the most probable I.P. obtained experimentally, whether or not the vibrational and rotational quantum numbers change. It is therefore usually assigned the value of the center of the appropriate peak in the spectrum.

The calculation of a complete ionization spectrum is beyond the present capabilities of DMC methods, since one must account for the effect of the generally large number of accessible final vibrational and rotational wave states. Each of these will give rise to an ionization process with a different energy and a different cross section. Calculation of the latter is important since it determines the shape of the spectrum, including the threshold energy at which ionization starts to occur and where the peak lies. The experiments are normally performed at room temperature; for silane and methane this means that initially the molecules are overwhelmingly likely to be in their lowest vibrational states. Consider what happens if the equilibrium geometries of the neutral and ionized molecules are well separated in configuration space. The cross section for a given transition is proportional to the square of the overlap of the vibrational parts of the wave functions of the initial and final states. As the

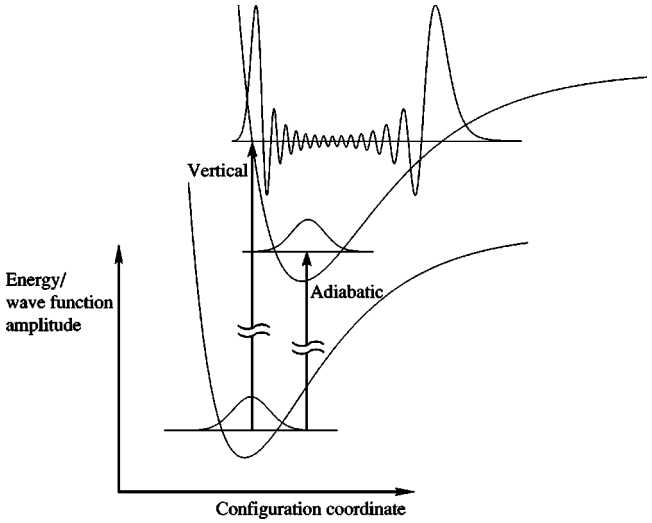

FIG. 1. A schematic of the (electronic) potential energy surfaces corresponding to the ground and singly ionized states of a molecule. Also shown are representations of the ground- and excited-state vibrational wave functions. The arrows indicate the definitions of the vertical and adiabatic ionization potentials as used in this paper.

final vibrational state is highly excited its vibrational wave function has a nearly classical distribution with most of its weight near the classical turning points. The most probable transitions are therefore to states vertically above the ground state on the configuration–coordinate diagram, see Fig. 1. Within this model the estimate of the vertical ionization energy is the difference between the excited- and ground-state electronic energies in the ground-state T_d configuration, *minus* the zero-point vibrational energy in the ground state, as shown in Fig. 1.

The theoretical interpretation of the adiabatic I.P. is also represented in Fig. 1. The adiabatic I.P. is the lowest possible energy needed to ionize the molecule and is therefore associated with the onset of the experimental spectrum. As Fig. 1 implies, the overlap of the vibrational parts of the wave functions is small if the minima in the two potential energy surfaces are well separated, and therefore the corresponding cross section will be small. If it is too small, then the onset of the spectrum will correspond to excitation into a slightly higher vibrational state which has a stronger overlap with the ground state of the neutral molecule. Hence, the theoretical value provides a lower bound on the adiabatic I.P.

TABLE II. Geometries obtained within LSDA-DFT for the C_s structure of SiH_4^+ and the C_{2v} and D_{2d} structures of CH_4^+. Bond lengths are in Angstroms and angles are in degrees.

	SiH_4^+	CH_4^+ (C_{2v})	CH_4^+ (D_{2d})
$X–H_1$	1.504	1.204	1.137
$X–H_2$	1.859	1.204	1.137
$X–H_3$	1.786	1.101	1.137
$X–H_4$	1.504	1.101	1.137
$H_1–X–H_2$	89.07	57.67	141.98
$H_1–X–H_3$	101.47	113.99	96.09
$H_1–X–H_4$	122.45	113.99	96.09
$H_2–X–H_4$	89.06	113.99	96.09
$H_3–X–H_4$	101.48	124.69	141.98

In calculating the adiabatic I.P., we relaxed the ionized molecules within LSDA-DFT. For silane we find a saddle point with D_{2d} symmetry and a minimum-energy structure with C_s symmetry. In methane we find two stable geometries, one with C_{2v} symmetry and the other with D_{2d} symmetry. Although the D_{2d} structure is 0.15 eV lower than the C_{2v} structure within LSDA-DFT, in DMC they are even closer in energy and differ by less than the statistical error bar of 0.1 eV. The geometries of these configurations, as well as that for the C_s structure of SiH_4^+, are given in Table II. We associate the difference in the total (including zero-point) energies of the ionized molecule in its minimum-energy configuration and the neutral molecule in the T_d structure with the adiabatic I.P.

The results for the adiabatic I.P.s quoted in Table III include the zero-point energies (calculated using a harmonic approximation within LSDA) of 0.806 and 0.746 eV for the equilibrium geometries of SiH_4 and SiH_4^+, respectively. The corresponding values for methane are 1.167 eV for the neutral ground state and 0.964 eV for the C_{2v} structure of CH_4^+. (The D_{2d} structure gives almost identical results.) Our value for the adiabatic I.P. of methane is in good agreement with the *GW* and DMC results of Grossman *et al.*[8] (Note that Grossman *et al.*[8] compare their vertical and adiabatic I.P.s with an old value of the vertical I.P. of methane which is significantly smaller than the values given by Pullen *et al.*[2]

TABLE III. The vertical and adiabatic first ionization potentials of silane and methane. The vertical I.P.s do not contain any corrections for vibrational effects while the adiabatic results include the LSDA-DFT zero-point energies in the neutral and ionized molecules. The two experimental values for each vertical I.P. refer to the double peaks in the spectra. All energies are in eV.

	SiH_4		CH_4	
	Vertical	Adiabatic (C_s)	Vertical	Adiabatic (C_{2v})
LSDA	12.13	10.74	13.97	12.45
DMC	12.85(3)	11.12(3)	14.38(7)	12.61(6)
MRD-CI[a]	12.72	···	···	···
GW[b]	12.7	···	14.3	12.5
DMC[b]	12.6(1)	···	14.3(1)	12.7(1)
Experiment[c]	12.36,12.85	11.66	13.62,14.32	12.78

[a]Chantranupong *et al.* (Ref. 6).
[b]Grossman *et al.* (Ref. 8).
[c]Photoelectron spectroscopy, Pullen *et al.* (Ref. 2).

When the proper comparisons are made their calculated values are in good agreement with experiment.) All of the calculated adiabatic I.P.s for both silane and methane are somewhat below the experimental values, in agreement with the point made earlier that the theoretical value is a lower bound on this I.P.

Experimentally, the photoelectron spectrum in the region of the first I.P. shows a double peak for both methane and silane.[2] The generally accepted explanation is that the double peak arises from a Jahn–Teller distortion of the ionized molecule,[2,4,5] whose ground state is triply degenerate in the T_d geometry. The Born–Oppenheimer separation of the electronic and nuclear degrees of freedom breaks down close to this geometry, and therefore the vertical approximation is not strictly valid. In addition, there may be significant structure in the vibrational spectra of the molecule which would render the simple vertical approximation inaccurate.

Our DMC results for the vertical I.P.s are also given in Table III. To allow direct comparison with other calculated values we have not subtracted the zero-point energy from these vertical I.P.s. Our DMC values for the vertical I.P.s of silane and methane are in good agreement with the all-electron multireference single- and double-excitation configuration interaction (MRD-CI) calculations, *GW*, and the other DMC results, but the LSDA gives smaller vertical I.P.s. All of the calculated vertical I.P.s lie between the two peaks of the experimental spectra, except for the LSDA result. If we subtract the zero-point vibrational energy of the neutral molecule from the calculated values (as described above) then the agreement with experiment is significantly worse. The reason for this is presumably the inapplicability of the vertical approximation.

C. Results for excited states

1. Silane

The absorption spectrum of silane shows three broad peaks at energies of 8.8, 9.7, and 10.7 eV.[3] The assignment of these peaks has been the subject of much debate,[3,6,46,47] with many workers concluding that they correspond to $2t_2 \rightarrow 4s$, $2t_2 \rightarrow 4p$ or $4d$, and $2t_2 \rightarrow 4d$ or $5s$, respectively, where the $2t_2$ state is the highest-occupied molecular orbital (HOMO). Chantranupong *et al.* performed accurate all-electron MRD-CI calculations for the excited states of silane. They found only two strong absorption peaks in the relevant energy range, corresponding to the $2t_2 \rightarrow 4s$ transition at an energy of 9.4 eV and three closely spaced transitions of $2t_2 \rightarrow 4d/5s$ character at 11.0–11.3 eV. These features are confirmed by our CIS and DMC calculations. (The *GW*-BSE calculations of Rohlfing *et al.*[7] found three strong absorption peaks in close correspondence with the experimental ones, but these calculations are now thought to be subject to revision.[8]) Chantranupong *et al.* suggested that the experimental peaks at 8.8 and 9.7 eV derive from a Jahn–Teller splitting of the triply degenerate $2t_2 \rightarrow 4s$ transition.

Results for the first few dipole-allowed (T_2 symmetry) singlet excited states of silane are shown in Table IV. In agreement with Chantranupong *et al.*,[6] we find a gap between the first two strongly optically allowed excitations of 1.99(2) eV in DMC (2.06 eV in CIS) which is much larger than the gap of approximately 0.8 eV between the first two peaks in the experimental spectrum.[3] This fact, combined with the similar splitting observed in the first ionization spectrum of silane, leads to the conclusion that the first excited state is also subject to a Jahn–Teller splitting and is hence responsible for the first two peaks in the spectrum. This first dipole-allowed excited state is of *s*-like character and hence we assign the first peak in the spectrum to the $2t_2 \rightarrow 4s$ transition, in agreement with previous studies.

TABLE IV. Assignment of the first few dipole-allowed (T_2 symmetry) singlet excited states in silane. The transition energies are calculated as differences in total electronic energies and do not contain any corrections for vibrational effects. The oscillator strengths of the transitions are denoted by f and all energies are in eV.

	$2t_2 \rightarrow 4s$	$2t_2 \rightarrow 4p$	$2t_2 \rightarrow 5s$	$2t_2 \rightarrow 4d$
f, CIS	0.2330	0.0036	0.2316	0.7641
CIS	9.819	11.214	11.879	12.886
DMC(CIS)	9.47(2)	10.61(2)	11.46(2)	11.54(2)
f, MRD-CI[a]	0.3382	0.0301	0.5628[b]	
MRD-CI[a]	9.414	10.488	11.305	11.046
Experiment[c]	8.9,9.7	···	10.7	···

[a]Chantranupong *et al.* (Ref. 6). The quoted values are averages of the near-degenerate results given in that work.
[b]Due to the near degeneracy of states in this region, this value is a combination of their separate oscillator strengths.
[c]Itoh *et al.* (Ref. 3).

The second bright (dipole-allowed) excitation that we find is unlikely to be observed experimentally since it has a very low oscillator strength in comparison to the other three in Table IV. The low oscillator strength stems from the *p*-like character of the initial and final orbitals; hence, we assign this to the $2t_2 \rightarrow 4p$ transition, in agreement with Chantranupong *et al.*[6]

Finally, the third and fourth bright singlets are found to be of *s*- and *d*-like character, respectively. They are therefore identified with the $2t_2 \rightarrow 5s$ and $2t_2 \rightarrow 4d$ transitions. Within DMC, these two excited states are very nearly degenerate, although their ordering is opposite to that found by Chantranupong *et al.*[6] The reason for this is that our DMC result for the $2t_2 \rightarrow 4d$ excitation energy is ~ 0.5 eV higher than was obtained in that work.

Having assigned the excited states, we analyze the accuracy of the CIS nodal surface and compare our results with those obtained using other methods. In order to gauge the quality of the CIS guiding wave functions, we have repeated the calculation of the first singlet and triplet excitations using the more accurate but much more expensive CASSCF method. For the results presented here, an active space of eight (spin-restricted) orbitals and six electrons was used. The guiding wave functions used in DMC were constructed from the 50 most significant Slater determinants in the resulting expansion, i.e., those with the largest expansion coefficients.

Table V lists results for the ground, first singlet, and first triplet excited states calculated using wave functions of increasing accuracy. Guiding wave functions generated using HF, LDA-DFT (not shown in the table), or CASSCF were all

TABLE V. The ground state and lowest singlet ($^1\Delta E_1$) and triplet ($^3\Delta E_1$) excitation energies in silane. The quoted HOMO–LUMO and CIS ground-state energies are the HF result. The pseudopotential of Stevens *et al.* (Ref. 38) was used for these calculations with the exception of the HOMO–LUMO calculation for which we used our HF pseudopotential (Ref. 35). The transition energies are calculated as differences in total electronic energies and do not contain any corrections for vibrational effects. All energies are in eV.

	Ground state	$^1\Delta E_1$	$^3\Delta E_1$
HOMO–LUMO[a]	−165.413	11.51(4)	11.46(4)
DMC(HOMO–LUMO)	−170.57(2)	10.59(5)	10.20(8)
CIS	−165.413	9.819	8.777
CASSCF	−166.946	9.284	8.821
DMC(CIS)	−170.57(2)	9.44(4)	8.85(4)
DMC(CASSCF)	−170.51(3)	9.44(5)	8.89(4)
DMC(CASSCF)[b]	−170.56(5)	9.1(1)	8.7(1)
Experiment	⋯	8.9,9.7[c]	8.7[d]

[a]HOMO to LUMO promotion preserving T_2 symmetry.
[b]Grossman *et al.* (Ref. 8) and private communication.
[c]From Itoh *et al.* (Ref. 3). The values refer to the two peaks in the experimental spectrum.
[d]Electron energy loss result from Curtis and Walker (Ref. 49).

found to give essentially the same *ground-state* DMC energy. This is despite the fact that the ground-state energy within CASSCF is 1.5 eV lower than that calculated within HF. Hence, the ground-state nodal structure is well described by a single Slater determinant.

The simplest method of constructing an excited-state wave function is to promote a single electron from the HOMO to the lowest-unoccupied molecular orbital (LUMO). Since both the HOMO and the LUMO are triply degenerate in silane and methane, we take a combination of the ground-state HF orbitals which preserves the T_2 symmetry of the first excited state. As can be seen in Table V, this wave function provides a poor description of both the singlet and triplet excited states, both when the energy is evaluated variationally and when it is used as a guiding wave function within DMC. Moving to CIS produces a large improvement in both the singlet and triplet states, but CASSCF does better still. This is especially true for the singlet state since the Pauli exchange in that case is not as significant as for the triplet; hence, there is more correlation energy to retrieve. However, the key point to note from the results in Table V is the near equality of the DMC results obtained when CIS or CASSCF is used to provide the guiding wave function, which establishes that their nodal surfaces are of comparable quality.

For comparison, Table V also contains the results of Grossman *et al.*,[8] who performed DMC calculations using a CASSCF guiding wave function. The origin of the 0.3(1) eV/0.2(1) eV disparities between their results and ours for the first singlet/triplet excitations is unclear: we have repeated our calculation (using the same pseudopotential as Grossman *et al.*[8]) for the triplet state using a CASSCF wave function generated with an active space containing 8 electrons and 13 orbitals and obtained a virtually identical result. We have also repeated the calculation using the correlation-consistent basis set employed by Grossman *et al.*[8] (excluding the *g* function from the Si basis) and obtained results essentially identical (all differences less than 0.05 eV) to those when our basis was used.

Finally, comparison with experiment shows that our results for the singlet excitation lie between the first two peaks of the spectrum, as would be expected if they are due to a Jahn–Teller splitting of this first excited state. Our result for the triplet is also in agreement with experiment. As we noted earlier for the vertical I.P.s, it may be more consistent to subtract the ground-state zero-point vibrational energy from the vertical excitation energies, but this does not improve the overall agreement with experiment.

In Table VI we collect all relevant results for the first few bright singlet excitations, the first dark singlet excitation, and the first triplet excitation. We include the values obtained using the TD-LDA method and the DMC energies calculated using those guiding wave functions. It can be seen that, whereas the CIS method overestimates the singlet exci-

TABLE VI. The first few excitation energies in silane, including the first dark (dipole-forbidden) singlet and first triplet states. The transition energies are calculated as differences in total electronic energies and do not contain any corrections for vibrational effects. All energies are in eV.

	Singlets					
	Bright ($^1T_2$)					
Rydberg assignment	4*s*	4*p*	5*s*	4*d*	Dark ($^1T_1$)	Triplet
CIS	9.819	11.214	11.879	12.886	10.879	8.817
TD-LDA	8.043	8.725	9.989	10.504	8.708	7.839
DMC(CIS)	9.47(2)	10.61(2)	11.46(2)	11.54(2)	9.72(2)	8.85(2)
DMC(TD-LDA)	9.42(3)	10.53(4)	11.31(3)	11.70(4)	10.10(3)	8.96(2)
MRD-CI[a]	9.414	10.488	11.305	11.046	10.114	9.011
DMC(CASSCF)[b]	9.1(1)	⋯	⋯	⋯	⋯	8.7(1)
GW-BSE[b]	9.2	⋯	⋯	⋯	⋯	8.5
Experiment	8.9,9.7[c]	⋯	10.7[d]	⋯	⋯	8.7[e]

[a]Chantranupong *et al.* (Ref. 6). The quoted values are averages of the near-degenerate results given in that work.
[b]Grossman *et al.* (Ref. 8).
[c]From Itoh *et al.* (Ref. 3). The values refer to the positions of the two peaks in the experimental spectrum.
[d]Itoh *et al.* (Ref. 3).
[e]Electron energy loss result from Curtis and Walker (Ref. 49).

TABLE VII. The first few excitation energies in methane, including the first dark (dipole-forbidden) singlet and first triplet states. The transition energies are calculated as differences in total electronic energies and do not contain any corrections for vibrational effects. The oscillator strengths of the transitions are denoted by *f* and all energies are in eV.

	Singlets					
	Bright ($^1T_2$)					
Rydberg assignment	3*s*	3*p*	4*s*	4*p*	Dark ($^1T_1$)	Triplet
f, CIS	0.1662	0.0042	0.0787	0.1121	0	0
CIS	10.952	12.254	13.127	13.238	12.241	10.135
f, TD-LDA	0.0726	0.0022	0.0138	0.0684	0	0
TD-LDA	9.053	9.867	9.969	10.833	9.855	8.891
DMC(CIS)	10.56(6)	11.70(6)	12.72(6)	12.75(6)	11.81(6)	10.18(6)
DMC(TD-LDA)	10.70(7)	12.11(8)	12.5(1)	12.55(8)	11.71(6)	10.16(8)
f, MRCI[a]	0.129	0.019	⋯	⋯	0	0
MRCI[a]	10.64	11.9	⋯	⋯	⋯	10.25
DMC(CASSCF)[b]	10.4(1)	⋯	⋯	⋯	⋯	10.1(1)
GW-BSE[b]	10.5	⋯	⋯	⋯	⋯	10.1
Experiment[c]	9.7,10.4[d]	11.08		11.6[e]	⋯	⋯

[a]Mebel *et al.* (Ref. 9).
[b]Grossman *et al.* (Ref. 8).
[c]UV absorption with an estimated uncertainty of ±10%, Lee and Chiang (Ref. 48).
[d]The values refer to the positions of the two peaks in the experimental spectrum.
[e]This energy was assigned to the $1t_2 \rightarrow 4s$ transition by Lee and Chiang (Ref. 48), but we find that the mixing of the MOs in the excited state is too strong to justify this assignment.

tation energies, the TD-LDA method generally underestimates them. For the triplet, the CIS result is very close to experiment while TD-LDA again gives an underestimate. However, using the TD-LDA guiding wave functions in DMC produces very similar results to those obtained with CIS guiding wave functions. Therefore, the nodal surfaces of the wave functions produced by these two methods are of very similar quality.

The DMC and *GW*-BSE results of Grossman *et al.*[8] are also given in Table VI. Both of these methods give excitation energies that are 0.2–0.3 eV lower than our DMC(CIS) results for both the singlet and triplet excited states. However, as discussed above, we have been unable to find an explanation for this.

We investigated the stability of the first singlet excited state by performing a geometry relaxation within CIS. The molecule was found to dissociate into SiH_2+H_2 with both product molecules being in singlet states since S_z is conserved. Using DMC, the dissociation energy for this process was calculated to be $-6.14(3)$ eV (including ground-state zero-point energies from LDA-DFT). In contrast, the ground state of silane is stable with a dissociation energy of 3.36(3) eV for this process. This is somewhat greater than the value of 2.51 eV found by Chantranupong *et al.*[6] The finite lifetime of the excited state is likely to be a contributing factor to the breadth of the peaks in the experimental absorption spectrum.[3]

2. Methane

It is generally accepted[46,48] that the first excited state of methane is subject to a Jahn–Teller splitting similar to that discussed for silane above. However, the calculations of Mebel *et al.*[9] have raised the possibility that the lowest two peaks in the absorption spectrum of methane arise from the vibrational structure associated with a single electronic excitation, rather than an excitation into two different electronic states. Our results for the first few electronic excitations of methane are given in Table VII. For the optically allowed singlets, the trends in the CIS and TD-LDA oscillator strengths and the DMC(CIS) and DMC(TD-LDA) excitation energies are in good agreement with the multireference CI calculations of Mebel *et al.*[9] The energy obtained for the first bright singlet is also in good agreement with the DMC and *GW*-BSE results of Grossman *et al.*[8] For each of the bright states, DMC(CIS) is a significant improvement over CIS with excitation energies that are consistently 0.4–0.5 eV lower. As in silane, the TD-LDA singlet excitation energies are much lower than those from CIS and significantly underestimate the experimental values.

For the first triplet excitation, the agreement between our DMC(CIS) and DMC(TD-LDA) results and the other theoretical results shown in Table VII is also good. In fact, the CIS method also performs well for this state but TD-LDA significantly underestimates the triplet energy.

Using the TD-LDA wave function within DMC again gives results that are very similar to those from DMC(CIS). Hence, the earlier conclusions that were reached on the relative quality of the nodal surfaces produced by the two methods in silane still hold.

Despite the good agreement between the results of the most reliable theoretical methods listed in Table VII (DMC, MRCI, and *GW*-BSE), all of the excitation energies for which there are corresponding experimental values are too high. We attribute these discrepancies to the use of the vertical approximation in the theoretical calculations.

Within CIS we find the first excited state of methane to be unstable to dissociation. However, this does not agree with the more accurate MRCI calculation of Mebel *et al.*,[9]

who found two stable geometries (corresponding to two different excited electronic states that are degenerate in the T_d structure)—one with C_s (but close to C_{3v}) symmetry and the other with C_{2v} symmetry. This stability to dissociation presumably contributes to the better definition of the peaks in the spectrum[48] as compared to the very broad peaks seen in the absorption spectrum of silane.[3]

IV. CONCLUSIONS

We have described the calculation of excited electronic states within DMC using guiding wave functions obtained with the CIS, TD-LDA, and CASSCF methods. Although the TD-LDA excitation energies are significantly smaller than the CIS ones, the DMC energies obtained using the CIS and TD-LDA guiding wave functions are very similar. These DMC energies are also comparable with those obtained using guiding wave functions from the more accurate but expensive CASSCF method. This is important because the CIS and TD-LDA methods are relatively inexpensive and could therefore be used to provide accurate guiding wave functions for DMC calculations of excitation energies in large molecules.

The lowest absorption energies of silane and methane are quite close to the ionization threshold, and the excitations are into Rydberg states. The ionization and absorption processes are therefore closely related. The origin of the double-peaked structure in the photoelectron spectra and the lowest two peaks resolved in the absorption spectra of silane and methane is most likely to be due to the Jahn–Teller splitting of the first ionized/excited state,[2,4,5] or possibly the vibrational structure associated with the ionized/excited state.[9] The presence of the Jahn–Teller distortion and the possibility of important effects from the vibrational structure complicates the comparison of theoretical results with measured vertical ionization and excitation energies. Presumably this explains why there are discrepancies between the theoretical and experimental results for the vertical transitions, while there is very good agreement between the most advanced theoretical calculations.

We therefore conclude that the DMC method, combined with suitable methods for generating excited-state guiding wave functions such as CIS, is a viable and potentially very accurate method for calculating the excited states of molecules.

ACKNOWLEDGMENTS

Financial support was provided by EPSRC (UK). Computational resources on a COMPAQ multiprocessor machine (Columbus cluster), provided by U.K. Computational Chemistry Facility at the Rutherford Appleton Laboratory (Admin.: Department of Chemistry, King's College London, Strand, London WC2R 2LS) are acknowledged. Some calculations were performed on the CRAY-T3E administered by CSAR at the University of Manchester.

[1] B. L. Hammond, W. A. Lester, Jr., and P. J. Reynolds, *Monte Carlo Methods in Ab Initio Quantum Chemistry* (World Scientific, Singapore, 1994).
[2] B. P. Pullen, T. A. Carlson, W. E. Moddeman, G. K. Schweitzer, W. E. Bull, and F. A. Grimm, J. Chem. Phys. **53**, 768 (1970).
[3] U. Itoh, Y. Toyoshima, and H. Onuki, J. Chem. Phys. **85**, 4867 (1986).
[4] R. F. Frey and E. R. Davidson, J. Chem. Phys. **89**, 4227 (1988).
[5] T. Kudo and S. Nagase, Chem. Phys. **122**, 233 (1988).
[6] L. Chantranupong, G. Hirsch, R. J. Buenker, and M. A. Dillon, Chem. Phys. **170**, 167 (1993).
[7] M. Rohlfing and S. G. Louie, Phys. Rev. Lett. **80**, 3320 (1998).
[8] J. C. Grossman, M. Rohlfing, L. Mitas, and S. G. Louie, Phys. Rev. Lett. **86**, 472 (2001).
[9] A. M. Mebel, S.-H. Lin, and C.-H. Chang, J. Chem. Phys. **106**, 2612 (1997).
[10] R. M. Grimes, B. L. Hammond, P. J. Reynolds, and W. A. Lester, Jr., J. Chem. Phys. **85**, 4749 (1986).
[11] A. Szabo and N. S. Ostlund, *Modern Quantum Chemistry: Introduction to Advanced Electronic Structure Theory* (Dover, NY, 1996).
[12] L. Hedin and S. Lundqvist, in *Solid State Physics*, edited by F. Seitz, D. Turnbull, and H. Ehrenreich (Academic, New York, 1969), Vol. 23, p. 1.
[13] G. Onida, L. Reining, R. W. Godby, R. Del Sole, and W. Andreoni, Phys. Rev. Lett. **75**, 818 (1995).
[14] E. Runge and E. K. U. Gross, Phys. Rev. Lett. **52**, 997 (1984).
[15] M. Petersilka, U. J. Gossmann, and E. K. U. Gross, Phys. Rev. Lett. **76**, 1212 (1996).
[16] E. K. U. Gross, J. F. Dobson, and M. Petersilka, in *Density Functional Theory*, edited by R. F. Nalewajski (Springer, Berlin, 1996).
[17] M. E. Casida, in *Recent Advances in Density Functional Methods, Part I*, edited by D. P. Chong (World Scientific, Singapore, 1995), p. 155.
[18] M. E. Casida, in *Recent Developments and Applications of Modern Density Functional Theory*, edited by J. M. Seminario (Elsevier Science, Amsterdam, 1996).
[19] I. Vasiliev, S. Öğüt, and J. R. Chelikowsky, Phys. Rev. Lett. **86**, 1813 (2001).
[20] J. B. Anderson, J. Chem. Phys. **65**, 4121 (1976).
[21] J. W. Moskowitz, K. E. Schmidt, M. A. Lee, and M. H. Kalos, J. Chem. Phys. **77**, 349 (1982).
[22] P. J. Reynolds, D. M. Ceperley, B. J. Alder, and W. A. Lester, Jr., J. Chem. Phys. **77**, 5593 (1982).
[23] W. M. C. Foulkes, R. Q. Hood, and R. J. Needs, Phys. Rev. B **60**, 4558 (1999).
[24] R. Jastrow, Phys. Rev. **98**, 1479 (1955).
[25] K. C. Huang, Master's thesis, University of Cambridge, 1999.
[26] T. Kato, Commun. Pure Appl. Math. **10**, 151 (1957).
[27] P. R. C. Kent, R. J. Needs, and G. Rajagopal, Phys. Rev. B **59**, 12344 (1999).
[28] C. J. Umrigar, K. G. Wilson, and J. W. Wilkins, Phys. Rev. Lett. **60**, 1719 (1988).
[29] J. B. Foresman, M. Head-Gordon, J. A. Pople, and M. J. Frisch, J. Phys. Chem. **96**, 135 (1992).
[30] P. E. M. Siegbahn, J. Almlöf, A. Heiberg, and B. O. Roos, J. Chem. Phys. **74**, 2384 (1981).
[31] R. E. Stratmann, G. E. Scuseria, and M. J. Frisch, J. Chem. Phys. **109**, 8218 (1998).
[32] M. E. Casida, C. Jamorski, K. C. Casida, and D. R. Salahub, J. Chem. Phys. **108**, 4439 (1998).
[33] S. M. Rothstein, in *Recent Advances in Quantum Monte Carlo*, edited by W. A. Lester, Jr. (World Scientific, Singapore, 1998), Chap. 10.
[34] N. Troullier and J. L. Martins, Phys. Rev. B **43**, 1993 (1991).
[35] Y. Lee, P. R. C. Kent, M. D. Towler, R. J. Needs, and G. Rajagopal, Phys. Rev. B **62**, 13347 (2000).
[36] W. Müller, J. Flesch, and W. Meyer, J. Chem. Phys. **80**, 3297 (1984).
[37] E. L. Shirley and R. M. Martin, Phys. Rev. B **47**, 15413 (1993).
[38] W. J. Stevens, H. Basch, and M. Krauss, J. Chem. Phys. **81**, 6026 (1984).
[39] M. J. Frisch, G. W. Trucks, H. B. Schlegel *et al.*, GAUSSIAN 98, Revision A.6, Gaussian, Inc., Pittsburgh, PA, 1998.
[40] R. J. Needs, G. Rajagopal, M. D. Towler, P. R. C. Kent, and A. J. Williamson, CASINO version 1.0 User's Manual, University of Cambridge, Cambridge, 2000.
[41] K. Ohno, H. Matsuura, Y. Endo, and E. Hirota, J. Mol. Spectrosc. **111**, 73 (1985).
[42] J. F. Stanton, Mol. Phys. **97**, 841 (1999), and references therein.

[43] C. W. Greeff and W. A. Lester, Jr., J. Chem. Phys. **106**, 6412 (1997).
[44] D. Feller and D. A. Dixon, J. Phys. Chem. A **103**, 6413 (1999).
[45] J. M. L. Martin, Chem. Phys. Lett. **273**, 98 (1997).
[46] M. B. Robin, *Higher Excited States of Polyatomic Molecules* (Academic, New York, 1974), Vol. 1.
[47] M. B. Robin, *Higher Excited States of Polyatomic Molecules* (Academic, New York, 1985), Vol. 3.
[48] L. C. Lee, J. Chem. Phys. **78**, 688 (1983).
[49] M. G. Curtis and I. C. Walker, J. Chem. Soc., Faraday Trans. **85**, 659 (1989).